Am J Cancer Res 2023;13(6):2644-2656
www.ajcr.us /ISSN:2156-6976/ajcr0147111

Original Article

Catalase as a novel drug target for metastatic castration-resistant prostate cancer

Frantzeska Giginis, Joshua Wang, Aaron Chavez, Manuela Martins-Green

Department of Cell, Molecular and Systems Biology, University of California, Riverside, CA, USA

Received October 19, 2022; Accepted January 2, 2023; Epub June 15, 2023; Published June 30, 2023

Abstract: Prostate Cancer (PCa) is the second most prevalent cancer in the world. Currently, most treatments for PCa involve Androgen Deprivation Therapy (ADT) which inhibits androgen-dependent tumor cell growth. When PCa is diagnosed early and is still Androgen Dependent, ADT is effective. However, this therapy is not effective for metastatic Castration-Resistant Prostate Cancer (mCRPC). Although the mechanism of becoming Castration-Resistant is not fully understood, it is known that high levels of oxidative stress (OS) are important for cancer suppression. Catalase is a very important enzyme in controlling OS levels. We hypothesized that catalase function is critical for the progression to mCRPC. To test this hypothesis, we used a CRISPR nickase system to create a catalase knockdown in PC3 cells, a mCRPC human-derived cell line. We obtained a $Cat^{+/-}$ knockdown cell line, which has approximately half of the transcripts for catalase, half of the protein levels, and half of catalase activity. The $Cat^{+/-}$ cells are also about twice as sensitive to H_2O_2 exposure compared to WT cells, migrate poorly, have low attachment to collagen, high attachment to Matrigel, and proliferate slowly. Using SCID mice for a xenograft model, we show that $Cat^{+/-}$ cells form smaller tumors than wild-type tumors with less collagen and no blood vessels. These results were validated via rescue experiments where functional catalase was reintroduced into the $Cat^{+/-}$ cells and the phenotypes were reversed. This study shows a novel role for catalase in deterring mCRPC development and points to a new potential drug target for mCRPC progression. Summary: Novel treatments for Metastatic Castration-Resistant Prostate Cancer are needed. By taking advantage of the sensitivity of tumor cells to oxidative stress (OS), reducing an enzyme, catalase, that decreases OS, has the potential to provide another target for Prostate Cancer therapy.

Keywords: Androgen receptor, CRISPR, oxidative stress, metastasis, drug resistance

Introduction

Prostate cancer (PCa) is the second leading cause of cancer-related deaths in American men, with 1 in 9 expected to be diagnosed in their lifetime [https://www.cancer.org/cancer/prostate-cancer/about/key-statistics.html]. Currently, most treatment strategies include Androgen Deprivation Therapy (ADT) which can either involve blocking the production of androgens, blocking the androgen receptor (AR) with agonists, or preventing the translocation of the AR from the cytoplasm to the nucleus where it acts as a transcription factor for pro-oncogenic genes [1]. However, this strategy is only effective in cases of Androgen-Dependent Prostate Cancer (ADPC). ADPC that has not metastasized typically has a positive response to this therapy, but in most cases, PCa will progress to a metastatic Castration-Resistant Phenotype (mCRPC) in 2-3 years [1]. CRPC can grow without the presence of androgens, and also tends to respond poorly to most other treatments, including more general proliferation-targeting cancer drugs such as docetaxel [2] because PCa cells divide slowly. Once CRPC metastasizes, the median survival is three years [3].

Discussions regarding the shift in aggression from ADPC to mCRPC have been focused on the upregulation of AR that acts as a transcription factor and turns on genes involved in PCa cell proliferation [4-6]. However, it has been shown that only about 20% of mCRPC have an increase of AR compared to ADPC [7]. In mCRPC, ADT drugs such as Leuprolide, that function to lower overall testosterone, fail because of the intracrine androgen synthesis by PCa cells [8, 9]. While Cytochrome P450 inhibiting drugs, such as abiraterone acetate, have shown promise to

extend mADPC survival by several months [10], this drug functions to block Androgen production and will not be effective for PCa that is entirely Hormone-Refractory. For mCRPC, an immunotherapy is available, sipuleucel-T, but is costly and only increases survival by about 4.5 months [11]. These findings point to the need for novel drug targets for the treatment of mCRPC.

Although the mechanism of Castration-Resistance is not entirely understood, it is known that oxidative stress is necessary for this aggressive phenotype to develop [7, 12, 13]. Tumor cells that are castration-resistant need a mechanism of evading cell death while there are overwhelming levels of Reactive Oxygen Species (ROS) in their microenvironment, generated from their persistent proliferative state [14]. The high levels of ROS create a microenvironment that could be used for new drug therapies because tumor cells will be more susceptible to ROS-mediated apoptosis than the cells in healthy tissues.

It has been observed that antioxidant enzymes are typically dysregulated in cancer [12, 13, 15-20]. For example, overexpression of catalase, the antioxidant enzyme required for detoxification of H_2O_2, has been observed in several cancers, [21-24] including PCa [18]. It has been reported that in a mouse sarcoma cell line, catalase "protects" tumor cells from H_2O_2 induced apoptosis [20]. Catalase suppression, either through natural products or the potent catalase inhibitor, 3-amino-1:2:4:-triazole (ATZ), has been shown to trigger apoptosis in various cancer cell lines including ovarian, breast, and gastric [16, 25], Given that targeting the AR receptor pathway has become an arms race against the rise of different mechanisms of resistance, we sought to take advantage of the increased oxidative stress in the tumor microenvironment by targeting catalase.

Therefore, we hypothesized that knocking down catalase in PC-3 cells, a CRPC cell line isolated from a human metastatic lesion in the bone, will reduce cell proliferation and tumor progression. Our study presents strong evidence that catalase reduces cell migration, proliferation, and tumor development making it a viable drug target opportunity for PCa management.

Materials and methods

Cell culture

The PC-3 cell line is an androgen-independent prostate cancer cell line that was purchased from American Type Cell Culture Collection (Manassas, VA). $Cat^{+/-}$ is a PC-3 cell line obtained in our laboratory that has a disrupted Catalase gene in one allele leading to 50% Catalase expression/production/activity. Both cell lines were cultured on 0.1% Collagen Coated Tissue Culture plates at 37°C with 5% CO_2 and in RPMI-1640 (Sigma R8758) supplemented with 10% FBS, and 1% Penicillin (100 IU/ml)-Streptomycin (100 µg/ml). Media renewal was done as needed about 2-3 times per week. Unless otherwise specified, cells were prepared to be assayed by seeding at 3.0×10^4 cells/cm^2 and grown to about 80% confluency.

CRISPR system

CRISPR Double Nickase expression plasmid and sgRNA expressing plasmid were purchased from Santa Cruz Biotech (sc-400353-NIC). The Nickase was chosen to reduce the probability of off-target effects. Cells were transfected with 2 µg of plasmid DNA using Lipofectamine 2000 Transfection Reagent (Thermofisher 11668027). After 24 hr cells that were successfully transfected were selected using puromycin treatment at 10 µg/ml. Selection media was maintained for 48 hours. Surviving cells were then plated in a 96-well plate at a density of 0.3 cells/well to ensure each well contained a colony derived from a single cell. The various colonies were cultured under normal conditions until they were screened via RT-qPCR or immunoblot. The following gRNA sequences were used in this kit: Plus Strand, Gttattacagtagggccccg, and Minus Strand: ggttaccagctccagtggt to lead the CRISPR-NIC enzyme to an appropriate region on the Catalase gene.

Immunoblot analysis

The cells were washed with PBS then lysed in Radioimmunoprecipitation assay buffer (RIPA: 10 mM NaCl, 50 mM Tris pH 7.5, 5 mM of EDTA, 1% NP40, 1% Sodium Deoxycholate, 0.1% SDSm pH 7.5) and centrifuged for 15 min at 10,000 × g to remove cell debris. The superna-

tants were removed and aliquoted for subsequent use. Protein concentrations were determined using the DC Protein Assay kit (Bio Rad). Samples were prepared to run on the gels by adding a loading buffer containing sodium dodecyl sulfate (SDS) and heating at 95°C for 3 min. Proteins were separated by size via 12% SDS-Polyacrylamide gel electrophoresis (PAGE) followed by an overnight 45V wet tank transfer system (Bio-Rad) onto a nitrocellulose membrane. Primary antibodies consisted of anti-catalase antibodies (Abcam ab16731) diluted 1:1000 and antibodies to the reference gene, Histone 3 (cell signaling cat #9717) diluted 1:1000. 2 Antibodies: Ms-Gt HRP (1:500); Rb-Gt HRP (1:2000) were purchased from ABCAM ab97023 and ab970, respectively.

Total RNA extraction

Cells lines were washed in PBS and directly lysed on the plate with Trizol Reagent (Thermofischer 15596026). RNA was purified from the Trizol solution by the manufacturer's protocol using Direct-zol Kit (Zymo R2051). Briefly, lysates were centrifuged at 12,000 × g for 5 min to remove cell debris. The supernatant was loaded onto a spin column and centrifuged for 1 min at 12,000 × g. Flow-through was discarded. A DNAse treatment was done using the DNAse I in DNA digestion buffer supplied in the kit. RNA wash buffer was loaded onto the column to remove remaining Trizol and wash the RNA. The wash step was repeated and RNA was eluded in 30 µl of DNAse/Rnase-Free water.

Real-time qPCR

cDNA was synthesized using 500 ng of RNA with the PrimeScript RT reagent Kit (Takara RR037A) according to the manufacturer's protocol. qPCR results were normalized to β-actin as a reference gene. 2 µl of cDNA templet were mixed with a 23 µl master mix containing 12.5 µl SYBR Green (Bio-Rad), and 150 nM of oligonucleotide primers. PCR was carried out in a Bio-Rad Biorad CFX Connect real-time PCR detection system (Bio-Rad, Hercules, CA). The thermal profile was 95°C for 2 min followed by 40 amplification cycles, consisting of denaturation at 95°C for 15 s, annealing at 60°C for 60 s. Fluorescence was recorded after every cycle for quantitation purposes. A melt curve analysis was used to verify a single product consisting of heating from 65°C-95 with increments of 0.5°C for 5 s. The following oligonucleotide sequences were designed using IDT primer quest and verified with NCBI Primer-Blast. Beta-actin *Forward* GCTAAGTCCTGCCCTCATTT *Reverse* GTACAGGTCTTTGCGGATGT Catalase: *Forward* CTGGGAGACGAGACACATAAAC *Reverse* TGGTCACTCCCTCTACATTCT.

Catalase activity

Catalase activity was determined in nmol/min/ml using a Catalase Activity kit (Cayman Chemicals 707002). Briefly, cells were washed twice with PBS, scraped, counted, and centrifuged for 5 min at 125 × g. The cells were then lysed in cold buffer (50 mM potassium phosphate, pH 7.0, containing 1 mM EDTA). According to manufacturer's protocol, activity was measured by incubating cell extract containing catalase with methanol which will produce formaldehyde in the presence of an optimal concentration of H_2O_2. Formaldehyde production can be measured by adding 4-amino-3-hydeazino-5-mercapto-1, 2, 4, triazole (Purpald) which changes from colorless to purple in the presence of aldehydes. The change in color was quantified using a Plate reader (BioTek, Winooski, VT) at 540 nm.

Cell proliferation

Cells were seeded in six-well plates at a cell density of 3.0×10^4 cells/cm^2. Each day, cells were washed with sterile 1 × PBS followed by trypsinization and counted using a hemocytometer.

H_2O_2 toxicity

Cells were seeded in six-well plates at a cell density of 3.0×10^4 cells/cm^2. One day post-seeding concentrations of 0 µM, 25 µM, 50 µM, and 100 µM were added to cells. H_2O_2 was diluted in sterile PBS, immediately before use, and added also with each media change. Each day, cells were washed with sterile 1 × PBS followed by trypsinization and counting to determine the effects of H_2O_2 on the growth rate of the cells.

Adhesion assay

PC-3 cells were plated on a collagen-coated 6-well plate at a density of 3.0×10^4 cells/cm^2 and allowed to grow to about 80% confluency. Media was aspirated and cells were washed

with PBS. A pre-warmed 0.25% Trypsin EDTA solution was added and the cells were allowed to detach at room temperature and under observation in the microscope. The required time needed for all the cells to detach was used to quantify cell adhesiveness.

Migration assay

Confluent (95-100%) WT PC3 cells and $Cat^{+/-}$ PC-3 cells, were wounded with a sterile pipette tip by making a scratch across the center of the plate. Cell migration was determined by measuring the distance between the wounded edge to the leading edge of migration at time points 0, 12, 24, 48 hr, post-wounding.

Xenograft

Experiments were approved by the Institutional Animal Care and Use Committee of the University of California, Riverside. Male immunodeficient SCID Mice (4-5 weeks old) were anesthetized and injected subcutaneously in the area of the prostate with 10^7 of WT or $Cat^{+/-}$ PC-3 cells in 100 µl of PBS. They were allowed to grow for 7 weeks. At 7 weeks, mice were euthanized, and tumors were photographed, weighed, volume was measured, and then prepared for histology.

Histology

Steps are performed at room temperature unless otherwise indicated. Each tumor was cut in half and incubated in 4% Paraformaldehyde overnight at 4°C on a rocker. Then the tissue was washed in PBS three times for 15 min with gentle shaking followed by incubation in 0.1 M Glycine in PBS for 30 min with gentle shaking. This was followed by incubation in a 15% sucrose solution for 4 hr at 4°C followed by overnight incubation in 30% sucrose at 4°C. Tissues were rinsed with PBS and embedded into Optimal cutting temperature compound (OCT) and frozen using a dry ice ethanol slush. 8-10 µm sections were prepared and then stained with Hematoxylin and Eosin or Mason Trichome as previously described [26].

Statistics

Differences between groups were assessed using a student's t-test in Graphpad Instat Software (Graphpad, La Jolla, CA, USA). Data is represented as mean +/- Standard Deviation represented as error bars. qPCR statistics was performed using CFX Maestro™ software (BioRad, Hercules, CA, USA) and displayed the data as ddCT +/- SEM as error bars.

Results

PC-3 cells are dependent on catalase for growth

We evaluated proliferation of WT PC-3 cells while under inhibition of catalase using a specific inhibitor of this enzyme, 3-Amino-1, 2, 4-triazole (ATZ) (Supplementary Figure 1). PC-3 cells were treated with 250 mM ATZ which is ½ of the LD50 of ATZ for this particular cell line. We found that over the span of 5 days, inhibition of catalase resulted in very low proliferation and survival. It is clear that after only 24 hours of growth with the inhibitor, PC3 cells do not grow well. This indicated that catalase is important for the growth of the PC3 cells and could become a potential target to slow tumor growth in Castration-Resistant Prostate Cancer Tumors.

Catalase knockdown results in altered cellular processes

Using a CRISPR Double Nickase system, we produced a clonal population of PC-3 cells in which the catalase gene was disrupted in one allele of the chromosome ($Cat^{+/-}$); (**Figure 1A**). The WT cells are the original PC3 cells purchased from ATCC. Because our sequencing results showed a 4 bp deletion, we anticipate a complete loss of functionality in this allele due to a frameshift mutation. As expected for a stable knockdown of $Cat^{+/-}$ we observed approximately a 50% reduction in catalase mRNA transcript (**Figure 1B**), protein levels (**Figure 1C**), and enzymatic activity (**Figure 1D**). The original gels for the gel shown in **Figure 1C** are shown in Supplementary Figures 2 and 3.

Given that high proliferation is a major hallmark of cancer, we determined whether the lower catalase expression and activity in the $Cat^{+/-}$ line leads to a decrease in cell proliferation. Using cell counting over a course of six days to determine proliferation levels, we found that $Cat^{+/-}$ cells show a lower number of cells as early as day two of growth, with significantly fewer cells on days 3, 5, and 6 (**Figure 2A**).

In order to show that the catalase knockdown cells are deficient in response to oxidative stress induced by H_2O_2 exposure, the growth

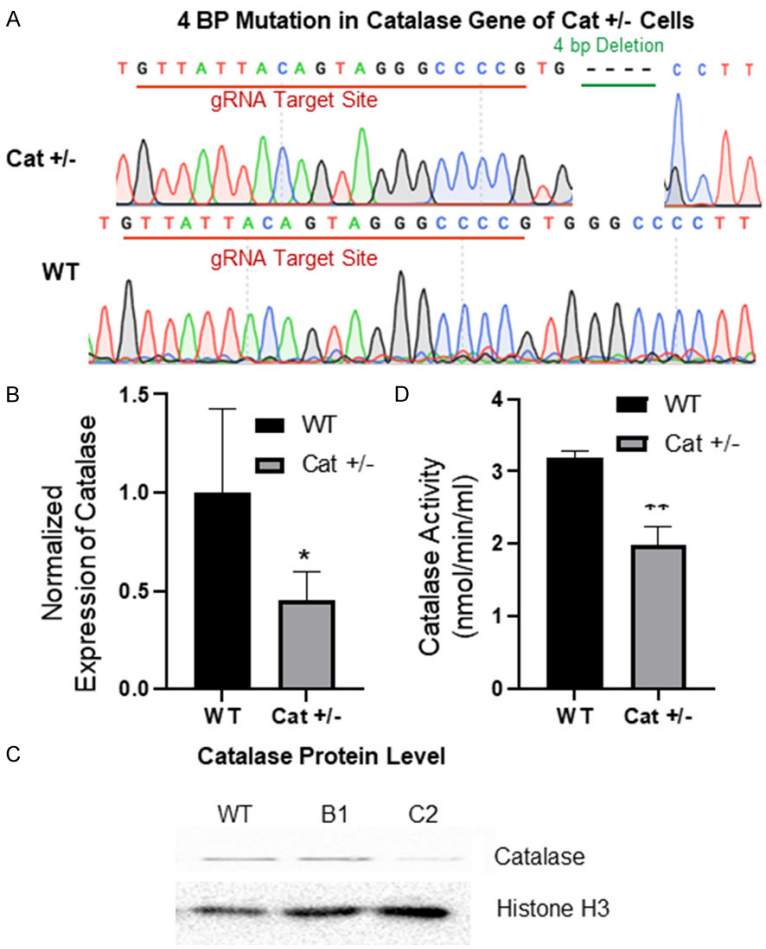

Figure 1. Catalase enzyme is successfully knocked down in PC-3 Cells. Verification of knockdown in a clonal PC-3 line done with various methods. A. Sanger sequencing of CRISPR target area revealing a 4 pb deletion. B. RT-PCR results showing decreased catalase mRNA levels. C. Western blot showing decreased catalase protein levels in two clonal populations after CRISPR. Clone "C2" was chosen for further screening of catalase activity loss. Clone "B1" did not have a lower catalase expression D. Catalase activity assay showing decreased catalase activity for the Cat$^{+/-}$ cells. All data are Mean ± Standard Deviation * = P< 0.05, ** = P<0.01, n = 3, 35 mm plates/time point.

curve was repeated with varying concentrations of H_2O_2 (**Figure 2B**). WT PC-3 cells exposed to 25 μM of H_2O_2 proliferated comparably to Cat$^{+/-}$ cell with no exposure to H_2O_2. When Cat$^{+/-}$ cells were exposed to any concentration of H_2O_2, there was a decreasing number of cells each day. In contrast, it required 50 μM of H_2O_2 treatment to induce similar levels of H_2O_2 toxicity in WT (**Figure 2B**).

Cat$^{+/-}$ cells also show perturbed adhesion. When plated on collagen, WT PC3 cells require over twice as long to fully become detached from the plate, showing that catalase loss decreases cell adhesion on collagen (**Figure 2C**). At room temperature, it requires about 11 min for WT to detach, whereas it takes about 5 min for Cat$^{+/-}$ cells to detach. In contrast, on Matrigel, Cat$^{+/-}$ cells show a slight, yet significant increase in adhesion compared to WT PC3 cells. At room temperature, PC3 cells detach from Matrigel in about 12 ½ min on average, whereas Cat$^{+/-}$ took about 17 min to detach (**Figure 2D**).

Another characteristic of cancer cells is the ability to migrate and metastasize. Migration can be evaluated *in vitro* by the scratch assay[26]. We plated the cells on collagen, made a scratch when the cells were confluent, and then compared the migration into the scratched space by the Cat$^{+/-}$ and the WT PC-3 by measuring the distance from the edge of the scratch to the front of the migrating cells at 12, 24, and 48 hr. Overall, Cat$^{+/-}$ cells migrate more slowly than WT (**Figure 3A**, **3B**). By the end of 48 hr, WT cells had migrated to completely close the gap, whereas Cat$^{+/-}$ cells had only migrated to about 50% closure (**Figure 3A**, **3B**).

When seeded in Matrigel, Cat$^{+/-}$ cells also show slower migration (**Figure 3C**, **3D**), although the difference between the WT and Cat$^{+/-}$ migration is not significant until 12 hr (**Figure 3D**). By 24, and 48 hr the migration of the Cat$^{+/-}$ cells is hindered even more on Matrigel than on collagen with WT cells closing the gap on average by 80% and Cat$^{+/-}$ cells closing the gap on average only 10% at 48 hr (**Figure 3D**).

Gain of catalase function reverses the altered cellular processes

To ensure that these observations are a direct result of catalase loss and not an off-target

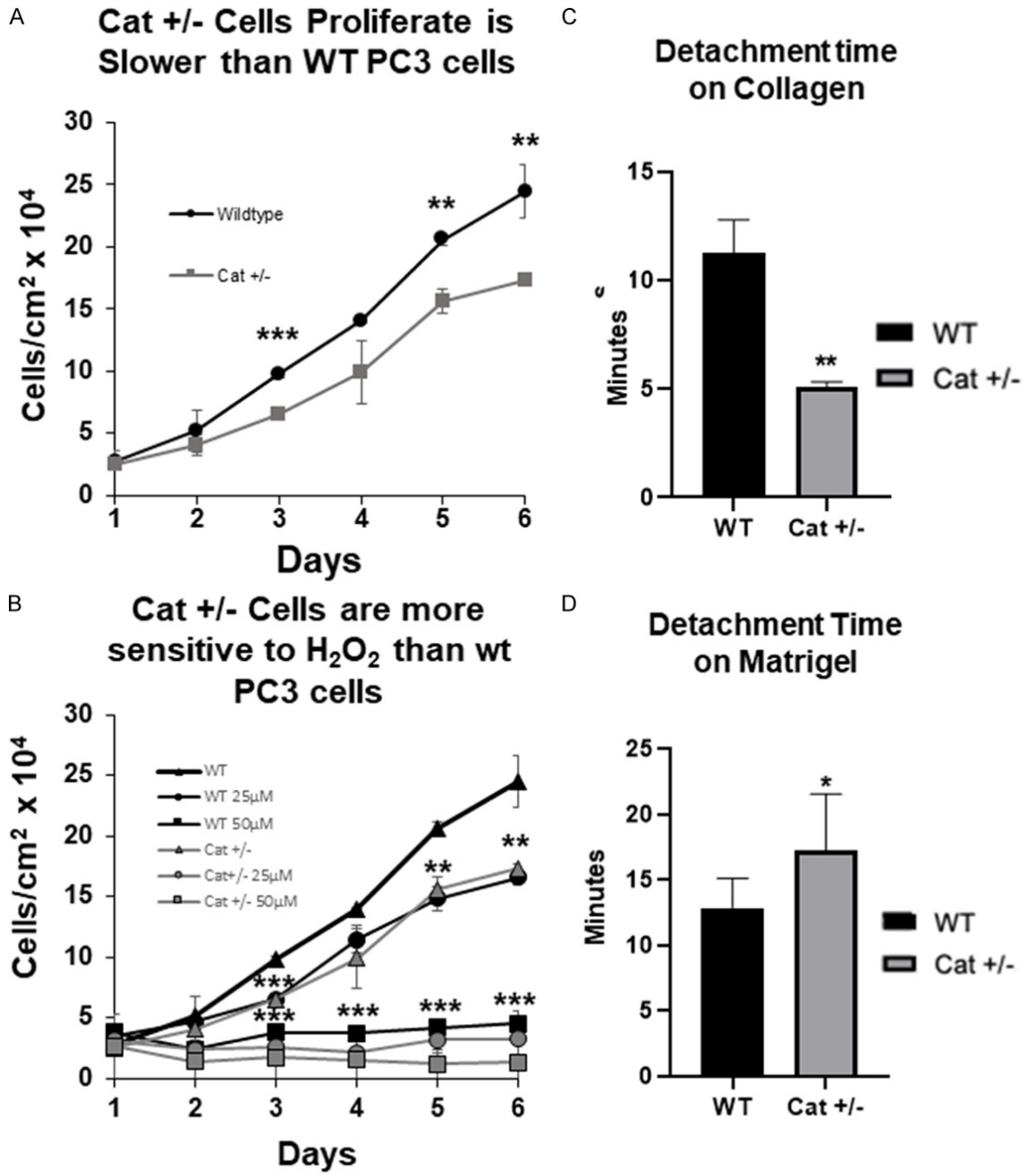

Figure 2. Catalase knockdown decreases proliferation, increases susceptibility to H_2O_2 toxicity, decreases adhesion on collagen, but increases adhesion on matrigel. A. $Cat^{+/-}$ cells proliferate slower compared to WT PC3 cells under standard growth conditions. B. $Cat^{+/-}$ cells are about twice as sensitive to H_2O_2 when compared to WT PC-3 cells. C. $Cat^{+/-}$ cells are less adhesive on Collagen then WTPC-3 cells. D. $Cat^{+/-}$ cells are more adhesive on Matrigel than WT PC-3 cells. All data are Mean ± Standard Deviation * = *P*< 0.05, ** = P<0.01, ** = P<0.001; n = 3, 35 mm plates/time point.

effect of the CRISPR system, we performed rescue experiments by stably transfecting a catalase expressing plasmid into the $Cat^{+/-}$ cell line. Successful transfection of the plasmid was validated via PCR amplification of the promoter region of the neomycin resistance cassette in transfected cells, but not in non-transfected cells (**Figure 4A**). To show that the plasmid is in fact expressing functional catalase, we also determined that there is increased

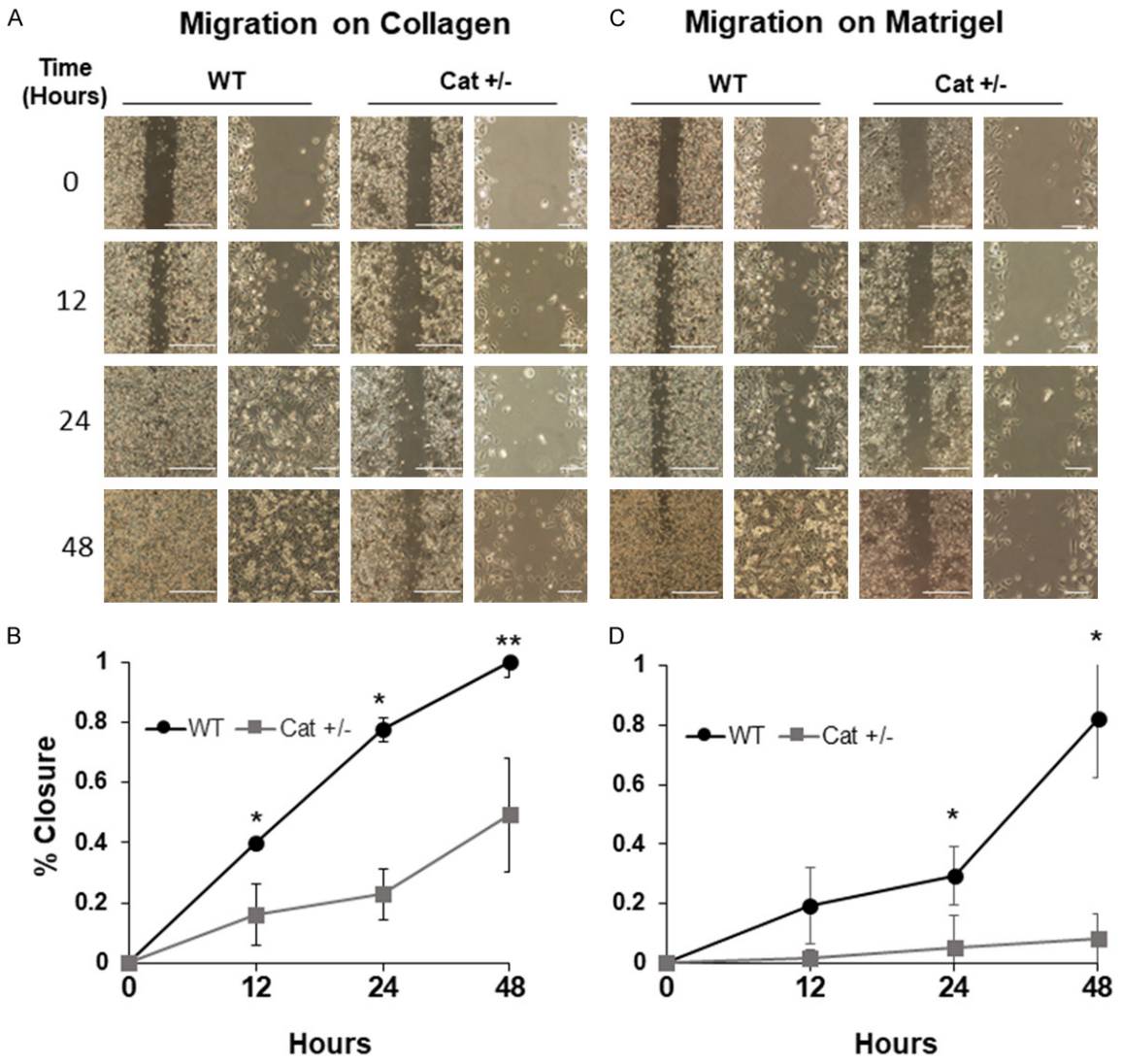

Figure 3. Catalase knockdown cells grown on collagen and matrigel have decreased migration in response to injury. $Cat^{+/-}$ cells and WT PC-3 cells were grown on 35 mm to complete confluency and then wounded. A. Slower percent closure over time was measured for $Cat^{+/-}$ cells on Collagen. Representative photos of $Cat^{+/-}$ and WT PC-3 cells migrating on Collagen. B. Quantitation of percent wound closure on collagen using image J. C. Representative photos of $Cat^{+/-}$ and WT PC-3 cells migrating on Matrigel. D. Quantitation of percent closure on matrigel using ImageJ. All data are Mean ± Standard Deviation * = $P< 0.05$, ** = $P<0.01$, n = 3, 35 mm plates/time point. Scale bars are 500 and 100 nm for lower and higher magnification, respectively.

catalase activity levels even compared to PC-3 cells (**Figure 4B**). This indicates that we have rescued catalase activity ($Rcat^{+/-}$).

We found that when Catalase was reintroduced into the cells, proliferation increased to become similar to the proliferation of WT PC3 cells (**Figure 4C**). Also, the alterations in adhesion we observed in the $Cat^{+/-}$ were reversed in the $RCat^{+/-}$ line. On collagen, the $RCat^{+/-}$ line showed a significant increase in adhesion compared to WT PC-3 cells (**Figure 4D**) whereas on Matrigel, the $RCat^{+/-}$ was not significantly different from WT PC-3 cells (**Figure 4E**). This latter result also shows that the plasmid used for transfection does not have secondary effects on the cells. In addition, we determined that $RCat^{+/-}$ migrated similarly to WT PC-3 cells (**Figure 5**). This occurs both on collagen (**Figure 5A**, **5B**) and Matrigel (**Figure 5C**, **5D**).

Catalase knockdown results in smaller tumor size in vivo

Although *in vitro* migration and proliferation assays can offer insight into tumor biology, to

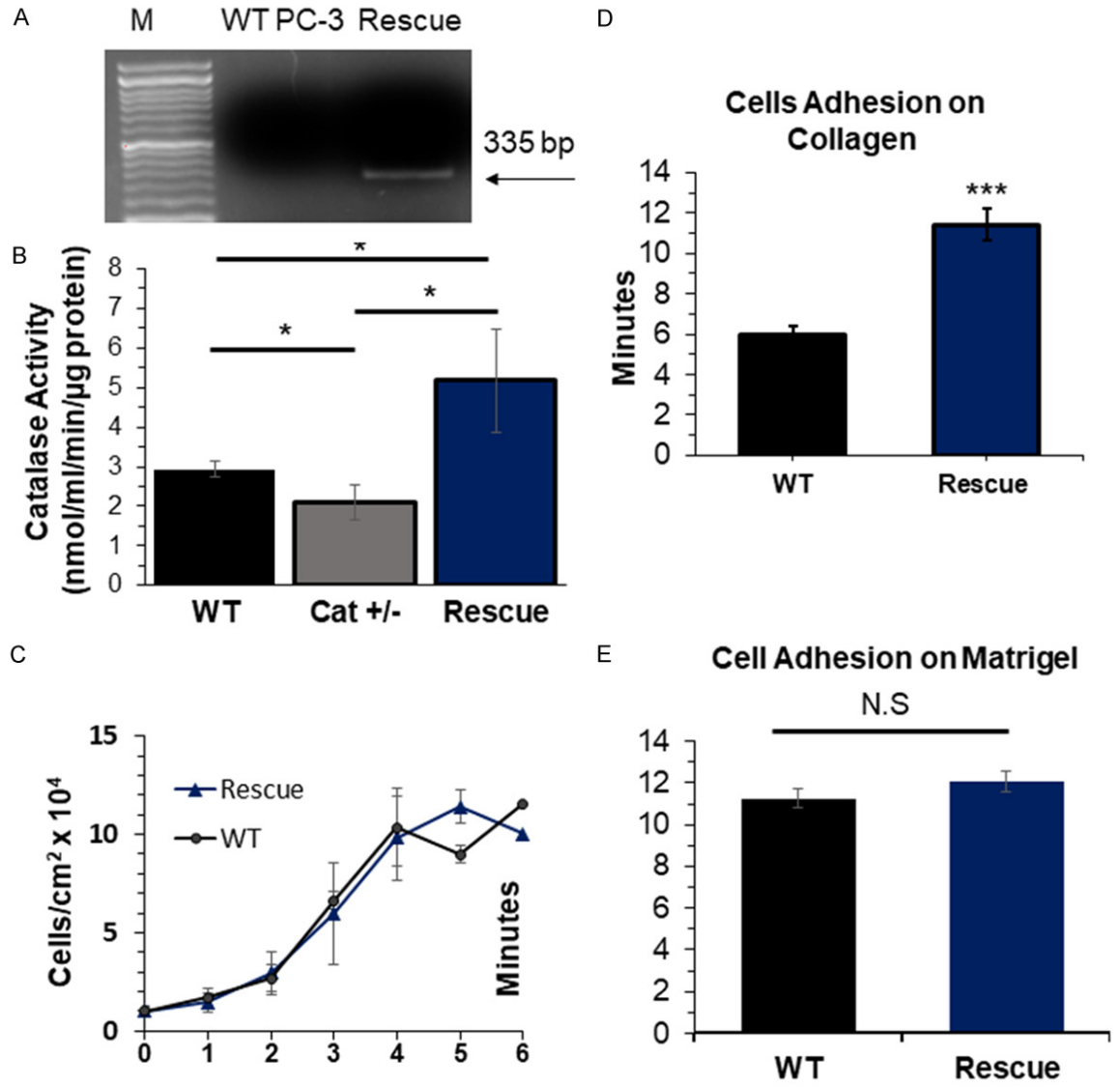

Figure 4. Catalase rescue was established in the knockdown background. A. PCR of Neomycin resistance gene in rescue plasmid only amplifies this gene in RCat$^{+/-}$ DNA. B. Catalase activity showing that RCat$^{+/-}$ has activity levels that equal to or exceed that in WT PC-3 cells. C. Cat$^{+/-}$ cells and WT PC-3 cells were grown on 35 mm dishes and proliferation was determined by counting. RCat$^{+/-}$ cells show a comparable rate of proliferation to WT PC-3. D. RCat$^{+/-}$ cells show even higher adhesion to collagen than WT PC-3 cells do. E. RCat$^{+/-}$ cells seeded on Matrigel have comparable adhesion to WT PC-3 cells. All data are Mean ± Standard Deviation * = P< 0.05, ** = P<0.01, ** = P<0.001; n = 3, 35 mm plates/time point.

determine whether catalase plays a role in prostate tumor growth, we used a xenograft model to examine whether there were differences in tumor growth *in vivo*. WT and Cat$^{+/-}$ PC-3 cells were xenografted into SCID immunodeficient mice. After 7 weeks of tumor growth, mice were euthanized, tumors were removed and then photographed showing that overall, Cat$^{+/-}$ cells formed significantly smaller tumors than WT PC3 cells (**Figure 6A**). All WT tumors had blood vessels indicated by blue arrows, whereas the Cat$^{+/-}$ tumors did not (**Figure 6A**). WT PC-3 cells-derived tumors weighed significantly more than tumors developed from Cat$^{+/-}$ tumors (**Figure 6B**). Also, WT PC3 cells-derived tumors had significantly larger volume than those developed from Cat$^{+/-}$ cells (**Figure 6C**).

To determine whether the decrease in tumor size generated by the Cat$^{+/-}$ cells was due to

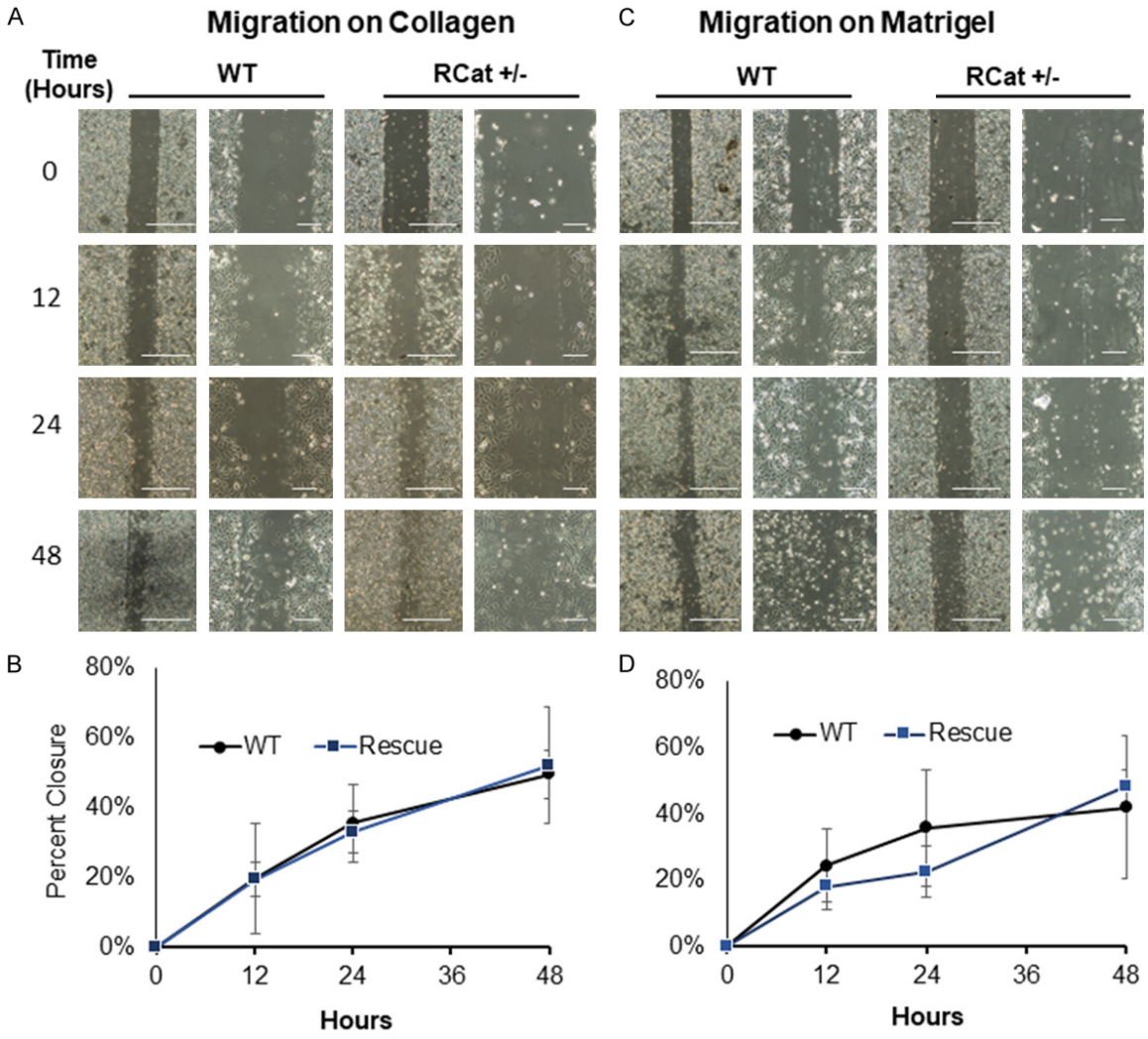

Figure 5. Catalase is responsible for decreased migration in response to injury. Percent closure was measured for RCat$^{+/-}$ cells cultures on (A, B) Collagen and (C, D) Matrigel. Representative photos of Rcat$^{+/-}$ Cells migrate in response to injury during a scratch assay slower than control WT cells on both (A, B) Collagen and (C, D) Matrigel. All data are Mean ± Standard Deviation, No significance; n = 3, 35 mm plates/time point. Scale bars are 500 and 100 nm for 4 × and 10 ×, respectively.

catalase loss, we performed xenografts experiments using the RCat$^{+/-}$ cell line and observed that the Rcat$^{+/-}$-derived tumors grew to a size between that of the tumors caused by the WT cells and the Cat$^{+/-}$ cells (**Figure 6A**). We also observed that the presence of blood vessel formation was similar to that of the WT xenografts. Xenografted tumors were also sectioned and stained with Hematoxylin and Eosin. Cat$^{+/-}$ tumors were more solid, whereas WT tumor showed evidence of necrosis in the center of the tumor (**Figure 6D**, arrowhead). In addition staining with Masson trichrome blue, showed that the Cat$^{+/-}$ tumors have very little collagen staining comparing with WT PC3 tumors (**Figure 6E**, arrowheads).

Discussion

When castration-resistant prostate cancer becomes metastatic there is a poor prognosis and therefore there is currently a need for novel therapeutic targets. As of right now, there is no reliable treatment for mCRPC. Drugs currently used at this stage of disease (such as enzalutamide and cabazitaxel, often called “third line treatments”) have severe side effects that can lead to discontinuation of use as well as a gen-

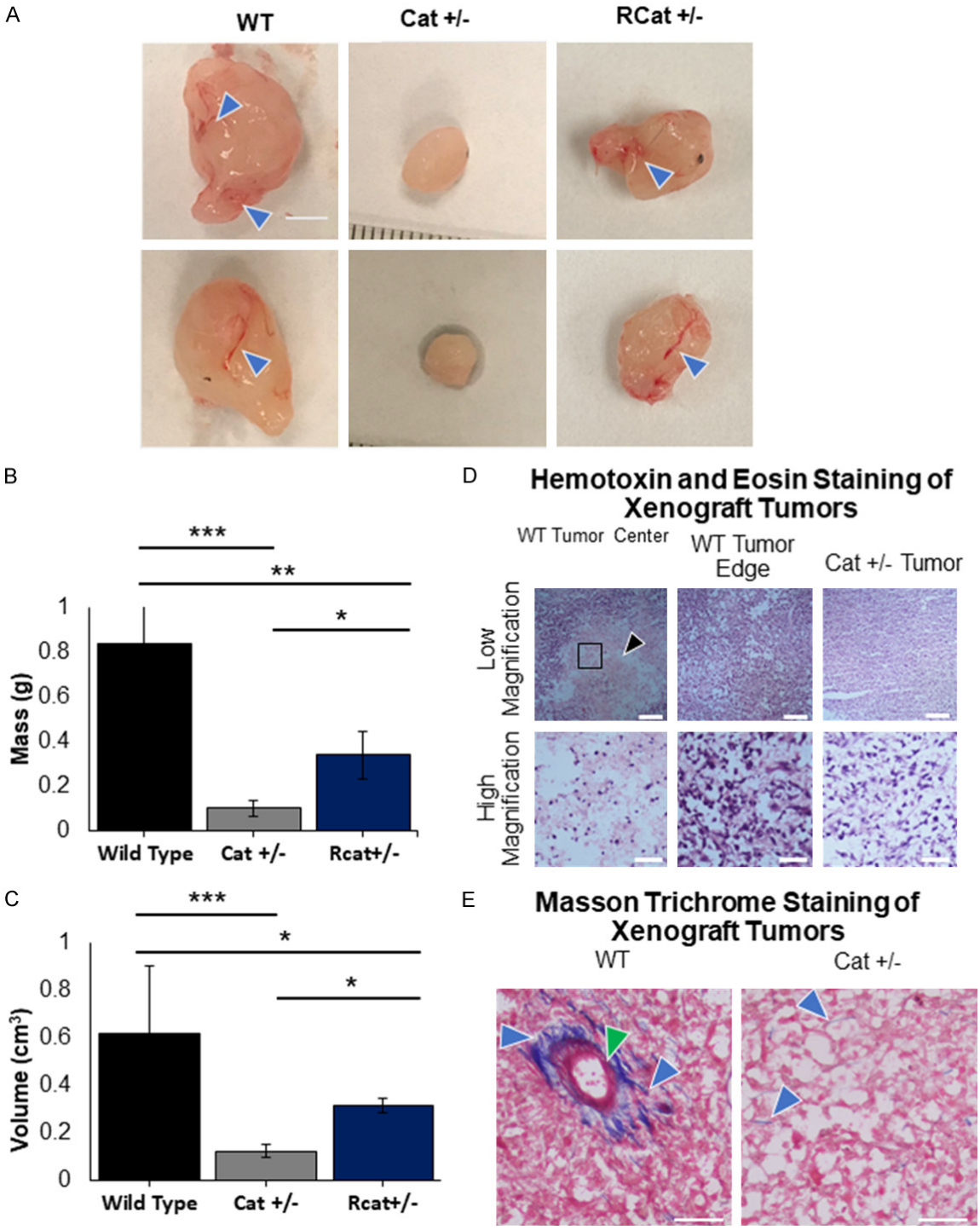

Figure 6. Catalase knockdown cells form smaller xenograft tumors and produce less collagen. When $Cat^{+/-}$ cells were Xenografted into immunodeficient SCID mice, they formed significantly smaller tumors. (A) Representative images of tumors. (B) Quantification of tumor mass. (C) Quantification of tumor volume. All data are Mean ± Standard Deviation * = $P< 0.05$, ** = $P<0.01$, ** = $P<0.001$. Tumors, $Cat^{+/-}$ n = 5, WT n=4 $RCat^{+/-}$ n = 5. Scale bar is 0.5 cm. Histological stains of xenograft tumors. Arrowheads show necrotic tumor center. Representative section of xenografted tumors are stained with Hematoxylin and Eosin (D) showing that the $Cat^{+/-}$ tumors are solid whereas the WT tumors show signs of cell death indicated by the black arrowhead. (E) Masson Trichrome staining of tumor sections show that $Cat^{+/-}$ xenografts contains less collagen indicated by blue arrowheads and fail to establish blood vessels as is the case with the WT tumors (green arrowhead). Scale bars are 100 and 50 μm for lower and higher magnification, respectively.

erally poor impact on serum PSA and overall survival [27, 28]. This point to the need for thinking outside of the typical Androgen-Receptor pathway for new drugs. In the work presented here, we identify the antioxidant enzyme, catalase, as a promising target for prostate cancer management. We used a cell line that is not only hormone-refractory but is also metastatic (derived from a metastasis in the human bone) [https://www.atcc.org/products/crl-1435] and an *in vivo* xenograft model to investigate the role of catalase in prostate cancer development. The sensitivity of tumor cell lines to ROS has been well characterized [29]. Prostate cancer cells specifically have been shown to be more sensitive to H_2O_2 mediated apoptosis [16, 17] leading us to consider catalase, an H_2O_2 scavenger, as a potential target for anti-cancer treatment.

In order to characterize prostate cancer progression with lower catalase activity, we established a CRISPR-Nickase (NIC)-mediated catalase knockdown in the mCRPC cell line (PC3). After confirmation of a four base-pair DNA deletion at the CRISPR gRNA target site in the catalase gene and of a decrease in catalase activity, we determined that this catalase knockdown cell line ($Cat^{+/-}$) was a good model to study tumorigenicity of mCRPC when catalase is suppressed. Consistently, we found that lower catalase expression resulted in reduction of processes critical for prostate cancer progression. We show that the mCRPC cell line deficient in catalase ($Cat^{+/-}$) in *in vitro* studies has: (i) 50% less catalase activity; (ii) reduced cell proliferation and migration; (iii) decreased cell adhesion to collagen; (iv) increased cell adhesion to matrigel, a basement membrane-like matrix; and (v) has much reduced growth *in vivo* during tumor development resulting in highly significant tumor volume, tumor weight and lack of blood vessels.

Increased cellular proliferation is a major hallmark of cancer [4]. We found that the $Cat^{+/-}$ cells proliferate slower than the wild-type cells. The rescue experiment confirmed that this decrease in proliferation is due to catalase loss. We also confirmed that the $Cat^{+/-}$ cells are half as sensitive to H_2O_2 as WT PC-3 cells. Given that WT PC-3 cells grow nearly as slowly as $Cat^{+/-}$ cells in the presence of 25 μM of H_2O_2, it is likely the $Cat^{+/-}$ cell line has lower proliferation in response to H_2O_2 accumulation. Consistent with what has previously been shown in other cancers, this is likely because cancer cells are already more sensitive to H_2O_2 [15-17]. Decreasing their ability to detoxify the microenvironment, will lead to an increase in cell death. Given that cells produce their own H_2O_2 and that cancer cells are known to produce more H_2O_2 than their tissue healthy counterparts [30], lowering catalase activity can lead to tumor destruction.

In addition to proliferation being an indicator for cancer progression, the ability to metastasize is an important hallmark of cancer [14]. One of the major steps in metastasis is the ability of the cancer cells to migrate through collagen-rich connective tissue towards blood vessels, adhere to the basement membrane, and enter blood vessels to travel to distant sites where the process is reversed. Our finding that $Cat^{+/-}$ do not adhere well and migrate much slower than the WT PC3 cells indicates that loss of catalase interferes with the expression of adhesion molecules, which are important in cell and molecular mechanisms of metastases. Because we were able to rescue the adhesion by re-expressing catalase, we know that it is catalase loss that is contributing to this phenotype.

Clinically, prostate cancer tumors exist in a three-dimensional environment therefore, we tested the ability of the $Cat^{+/-}$ cells to form solid tumors in a xenograft model. We found that $Cat^{+/-}$ cell tumors were significantly smaller in weight and volume compared to WT tumors, indicating that catalase loss leads to significant inhibition of tumor growth *in vivo*. Not only did catalase suppression lead to lower proliferation of the cancer cells in culture, but it also slowed the growth of a solid tumor. Furthermore, the $Cat^{+/-}$ tumors also had fewer blood vessels, decreasing their ability to obtain O_2 and nutrients needed to progress aggressively or metastasize. Angiogenesis is a major hallmark of cancer [4, 31]. Although the tumors-derived form our rescue $Cat^{+/-}$ cells ($Rcat^{+/-}$) did not reach the same size as WT, they did have the increase in blood vessels we see in WT tumors. Decreased angiogenesis is typically associated with less aggressive cancer because tumor cells are unable to maintain the nutrients needed for sustained growth and proliferation, and have fewer microvessels available to metastasize [4, 31]. Upon further inves-

tigation, we found that our rescue plasmid does not overexpress catalase in the tumor xenograft model to the same extent it does in cell culture conditions (data not shown).

Staining of tumor sections showed that the $Cat^{+/-}$ cells-derived tumors have much less collagen than the WT PC3 cells-derived tumors. High collagen density in tumors is generally associated with poor prognosis [32, 33] therefore a lower density of collagen is a characteristic of a less aggressive tumor. High amounts of collagen also can contribute to hypoxic conditions in tumors, signaling for increases in aggression and angiogenesis [32, 33]. Recent studies have shown that higher levels of collagen in tumors result in lower T-cell infiltration in breast cancer, so reduction in collagen may be even more important in cancer management than previously thought [32, 33].

In conclusion, we show here that catalase is a potential target for Metastatic Castration-Resistant Prostate Cancer. Stable knockdown of catalase results in slower-growing cancer cells that are more susceptible to H_2O_2 mediated cell death. Catalase deficient tumor cells show several phenotypes of a cancer that will migrate and metastasize very poorly. We are currently investigating the impact that catalase loss has on adhesion to different cell culture substrates. Overall, catalase reduction leads to suppression of progression of Prostate Cancer in both *in vitro* and *in vivo*.

Acknowledgements

We would like to acknowledge Dr. Collins from the Institute for Integrative Genome Biology at UC Riverside for technical support and sequencing and Yangtao Lin for helping in the submission of this manuscript.

Disclosure of conflict of interest

None.

Address correspondence to: Manuela Martins-Green, Department of Molecular, Cell and Systems Biology University of California Riverside Riverside, CA, USA. Tel: 1-951-827-2585; Fax: 1-951-827-3087; E-mail: manuela.martins@ucr.edu

References

[1] Harris WP, Mostaghel EA, Nelson PS and Montgomery B. Androgen deprivation therapy: progress in understanding mechanisms of resistance and optimizing androgen depletion. Nat Clin Pract Urol 2009; 6: 76-85.

[2] Bumbaca B and Li W. Taxane resistance in castration-resistant prostate cancer: mechanisms and therapeutic strategies. Acta Pharm Sin B 2018; 8: 518-529.

[3] Alpajaro SIR, Harris JAK and Evans CP. Non-metastatic castration resistant prostate cancer: a review of current and emerging medical therapies. Prostate Cancer Prostatic Dis 2019; 22: 16-23.

[4] Hanahan D and Weinberg RA. Hallmarks of cancer: the next generation. Cell 2011; 144: 646-74.

[5] Shiota M, Yokomizo A, Tada Y, Inokuchi J, Kashiwagi E, Masubuchi D, Eto M, Uchiumi T and Naito S. Castration resistance of prostate cancer cells caused by castration-induced oxidative stress through Twist1 and androgen receptor overexpression. Oncogene 2010; 29: 237-50.

[6] Linja MJ, Savinainen KJ, Saramäki OR, Tammela TL, Vessella RL and Visakorpi T. Amplification and overexpression of androgen receptor gene in hormone-refractory prostate cancer. Cancer Res 2001; 61: 3550-5.

[7] Shiota M, Yokomizo A and Naito S. Oxidative stress and androgen receptor signaling in the development and progression of castration-resistant prostate cancer. Free Radic Biol Med 2011; 51: 1320-8.

[8] Hamid ARAH, Tendi W, Sesari SS, Mochtar CA, Umbas R, Verhaegh G and Schalken JA. The importance of targeting intracrinology in prostate cancer management. World J Urol 2019; 37: 751-757.

[9] Sharifi N. Minireview: androgen metabolism in castration-resistant prostate cancer. Mol Endocrinol 2013; 27: 708-714.

[10] Attard G, Reid AH, A'Hern R, Parker C, Oommen NB, Folkerd E, Messiou C, Molife LR, Maier G, Thompson E, Olmos D, Sinha R, Lee G, Dowsett M, Kaye SB, Dearnaley D, Kheoh T, Molina A and de Bono JS. Selective inhibition of CYP17 with abiraterone acetate is highly active in the treatment of castration-resistant prostate cancer. J Clin Oncol 2009; 27: 3742-8.

[11] Anassi E and Ndefo UA. Sipuleucel-T (provenge) injection: the first immunotherapy agent (vaccine) for hormone-refractory prostate cancer. P T 2011; 36: 197-202.

[12] Khandrika L, Kumar B, Koul S, Maroni P and Koul HK. Oxidative stress in prostate cancer. Cancer Lett 2009; 282: 125-36.

[13] Kumar B, Koul S, Khandrika L, Meacham RB and Koul HK. Oxidative stress is inherent in prostate cancer cells and is required for aggressive phenotype. Cancer Res 2008; 68: 1777-85.

[14] Hanahan D and Weinberg RA. The hallmarks of cancer. Cell 2000; 100: 57-70.
[15] Doskey CM, Buranasudja V, Wagner BA, Wilkes JG, Du J, Cullen JJ and Buettner GR. Tumor cells have decreased ability to metabolize H2O2: implications for pharmacological ascorbate in cancer therapy. Redox Biol 2016; 10: 274-284.
[16] Bechtel W and Bauer G. Catalase protects tumor cells from apoptosis induction by intercellular ROS signaling. Anticancer Res 2009; 29: 4541-57.
[17] López-Lázaro M. Dual role of hydrogen peroxide in cancer: possible relevance to cancer chemoprevention and therapy. Cancer Lett 2007; 252: 1-8.
[18] Jung K, Seidel B, Rudolph B, Lein M, Cronauer MV, Henke W, Hampel G, Schnorr D and Loening SA. Antioxidant enzymes in malignant prostate cell lines and in primary cultured prostatic cells. Free Radic Biol Med 1997; 23: 127-33.
[19] Jia P, Dai C, Cao P, Sun D, Ouyang R and Miao Y. The role of reactive oxygen species in tumor treatment. RSC Adv 2020; 10: 7740-7750.
[20] Heinzelmann S and Bauer G. Multiple protective functions of catalase against intercellular apoptosis-inducing ROS signaling of human tumor cells. Biol Chem 2010; 391: 675-93.
[21] Hwang TS, Choi HK and Han HS. Differential expression of manganese superoxide dismutase, copper/zinc superoxide dismutase, and catalase in gastric adenocarcinoma and normal gastric mucosa. Eur J Surg Oncol 2007; 33: 474-9.
[22] Rainis T, Maor I, Lanir A, Shnizer S and Lavy A. Enhanced oxidative stress and leucocyte activation in neoplastic tissues of the colon. Dig Dis Sci 2007; 52: 526-30.
[23] Sander CS, Hamm F, Elsner P and Thiele JJ. Oxidative stress in malignant melanoma and non-melanoma skin cancer. Br J Dermatol 2003; 148: 913-22.
[24] Zelen I, Djurdjevic P, Popovic S, Stojanovic M, Jakovljevic V, Radivojevic S, Baskic D and Arsenijevic N. Antioxidant enzymes activities and plasma levels of oxidative stress markers in B-chronic lymphocytic leukemia patients. J BUON 2010; 15: 330-6.
[25] Yang L, Zheng XL, Sun H, Zhong YJ, Wang Q, He HN, Shi XW, Zhou B, Li JK, Lin Y, Zhang L and Wang X. Catalase suppression-mediated H(2)O(2) accumulation in cancer cells by wogonin effectively blocks tumor necrosis factor-induced NF-κB activation and sensitizes apoptosis. Cancer Sci 2011; 102: 870-6.
[26] Dhall S, Do DC, Garcia M, Kim J, Mirebrahim SH, Lyubovitsky J, Lonardi S, Nothnagel EA, Schiller N and Martins-Green M. Generating and reversing chronic wounds in diabetic mice by manipulating wound redox parameters. J Diabetes Res 2014; 2014: 562625.
[27] Chung DY, Kang DH, Kim JW, Kim DK, Lee JY, Hong CH and Cho KS. Comparison of oncologic outcomes between two alternative sequences with abiraterone acetate and enzalutamide in patients with metastatic castration-resistant prostate cancer: a systematic review and meta-analysis. Cancers 2019; 12: 8.
[28] von Eyben FE, Roviello G, Kiljunen T, Uprimny C, Virgolini I, Kairemo K and Joensuu T. Third-line treatment and 177Lu-PSMA radioligand therapy of metastatic castration-resistant prostate cancer: a systematic review. Eur J Nucl Med Mol Imaging 2018; 45: 496-508.
[29] Liou GY and Storz P. Reactive oxygen species in cancer. Free Radic Res 2010; 44: 479-96.
[30] Lennicke C, Rahn J, Lichtenfels R, Wessjohann LA and Seliger B. Hydrogen peroxide - production, fate and role in redox signaling of tumor cells. Cell Commun Signal 2015; 13: 39.
[31] Nishida N, Yano H, Nishida T, Kamura T and Kojiro M. Angiogenesis in cancer. Vasc Health Risk Manag 2006; 2: 213-9.
[32] Xu S, Xu H, Wang W, Li S, Li H, Li TJ, Zhang W, Yu X and Liu L. The role of collagen in cancer: from bench to bedside. J Transl Med 2019; 17: 309.
[33] Fang M, Yuan J, Peng C and Li Y. Collagen as a double-edged sword in tumor progression. Tumour Biol 2014; 35: 2871-82.

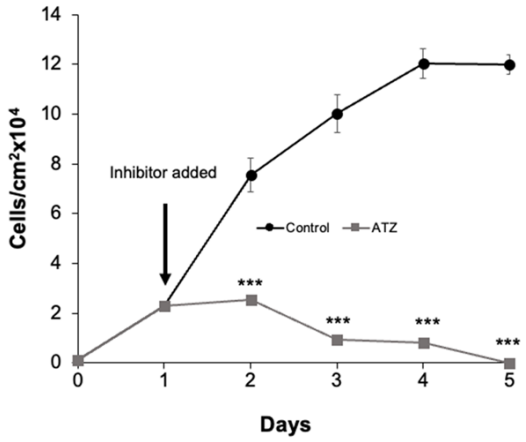

Supplementary Figure 1. Catalase Inhibition Catalase Inhibition Proliferation.

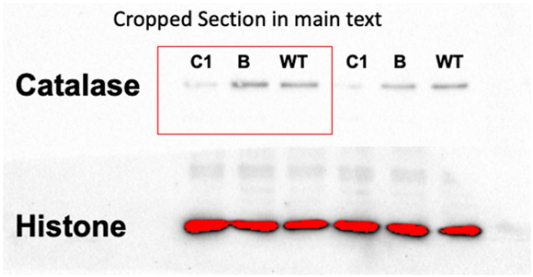

Supplementary Figure 2. Full length of **Figure 1C** Catalase Blot.

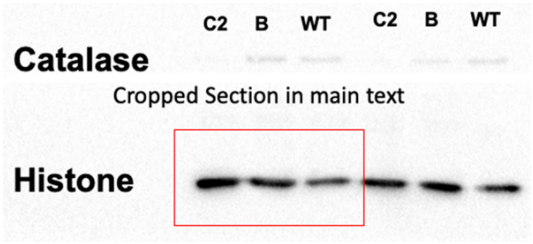

Supplementary Figure 3. Full length of **Figure 1C** Histone Blot.